Appendix 1

Methods

Tissue samples and IHC

Twenty-five pairs of esophageal squamous cell carcinoma tissue and adjacent normal tissue were collected from patients attending the First Affiliated Hospital of Zhengzhou University between May 2020 and February 2021. These samples were subjected to immunohistochemistry (IHC) analysis.

The tissue samples were fixed using 10% neutral buffered formalin and cut into tissue sample blocks with paraffin wax. The samples were subsequently sent to Wuhan Servicebio Biotech Co., Ltd. (China) to construct tissue microarrays (TMAs). The TMAs were incubated with an HTF9C (1:200; 16199-1-AP; Proteintech Group, Inc., China), PDHE1 Alpha (1:300; 18068-1-AP; Proteintech Group, Inc., China), MPRIP (1:300; 20040-1-AP; Proteintech Group, Inc., China), HSP70 (1:300; 10995-1-AP; Proteintech Group, Inc., China), Histone H4 (1:500; 16047-1-AP; Proteintech Group, Inc., China), IL-17A (1:500; 66148-1-AP; Proteintech Group, Inc., China) and KRI1 (1:400; bs-16814R; Beijing Biosynthesis Biotechnology Co., Ltd.) monoclonal antibody at 4 ℃ overnight. The TMAs were washed the next morning and incubated with a secondary antibody (GB23303, Servicebio, China) for 30 min at 37 ℃. Diaminobenzene was used as the chromogen, and hematoxylin was used as the nuclear counterstain. The immunostaining intensity of AUP1 was measured based on the H-score. The modified H-score (percentage of weak intensity ×1) + (percentage of moderate intensity ×2) + (percentage of strong intensity ×3) was used to determine the overall percentage of AUP1-positive cells across the entire stained tumor sample.

https://dx.doi.org/10.21037/tcr-2024-2561

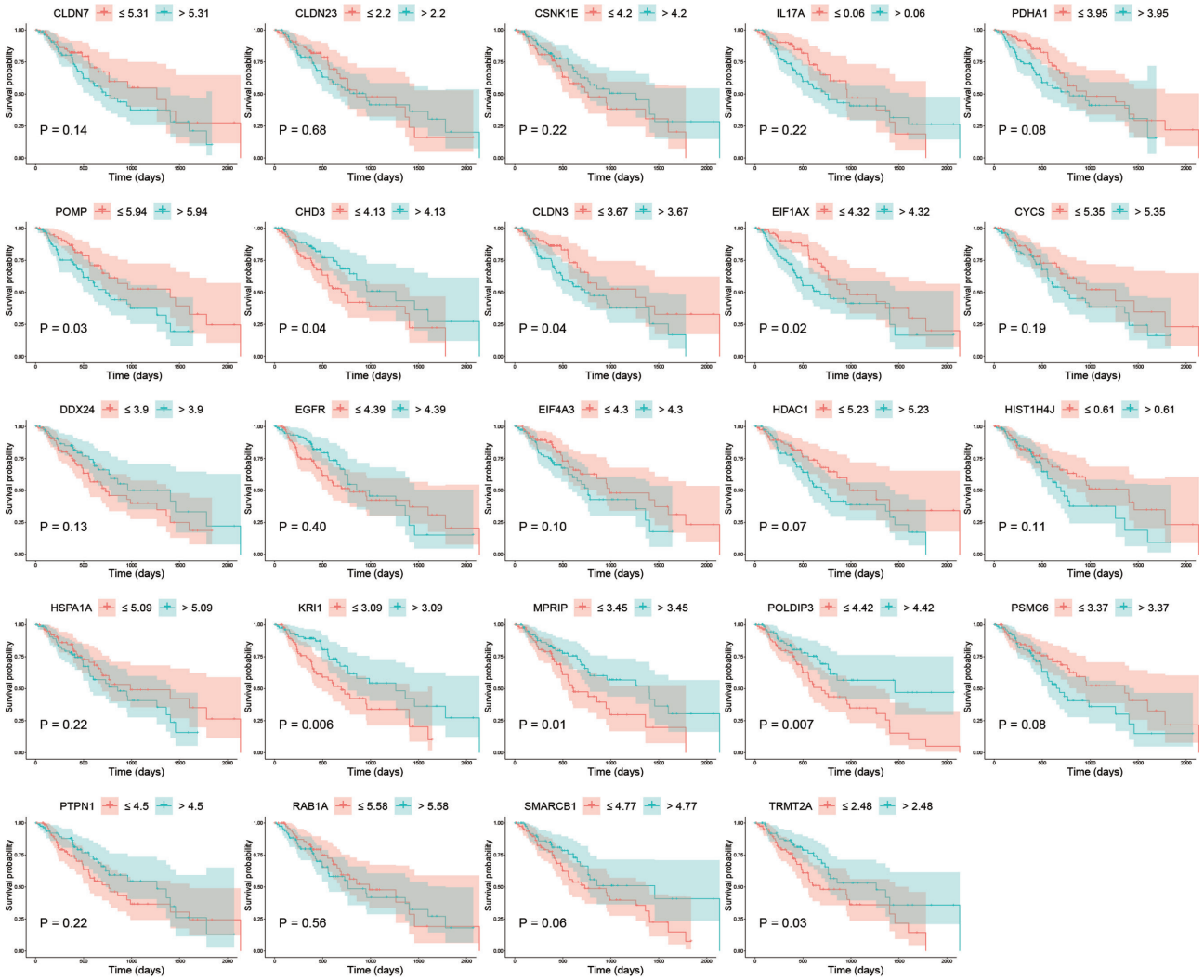

Figure S1 Prognostic value of hub genes in patients with esophageal cancer (Kaplan-Meier plots of CLDN7, CLDN23, CSNK1E, IL17A, PDHA1, POMP, CHD3, CLDN3, EIF1AX, CYCS, DDX24, EGFR, EIF4A3, HDAC1, HIST1H4J, HSPA1A, KRI1, MRIPP, POLDIP3, PSMC6, PTPN1, RAB1A, SMARCB1, TRMT2A grouped by median expression values).

https://dx.doi.org/10.21037/tcr-2024-2561

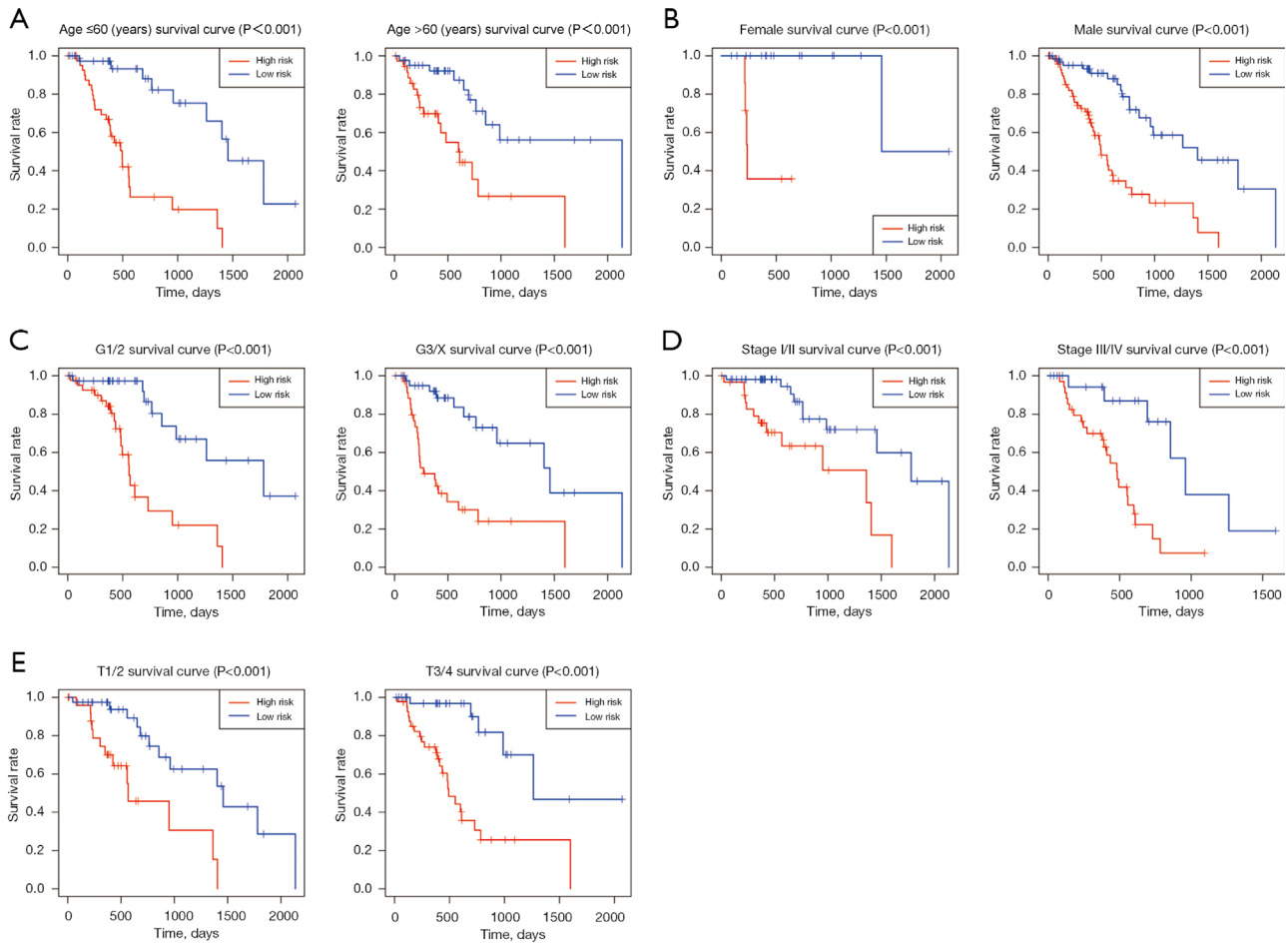

Figure S2 Verification of the prognostic value in different clinical subgroups. (A) Age. (B) Gender. (C) Histological grade. (D) Pathological stage. (E) Pathological T stage.

https://dx.doi.org/10.21037/tcr-2024-2561

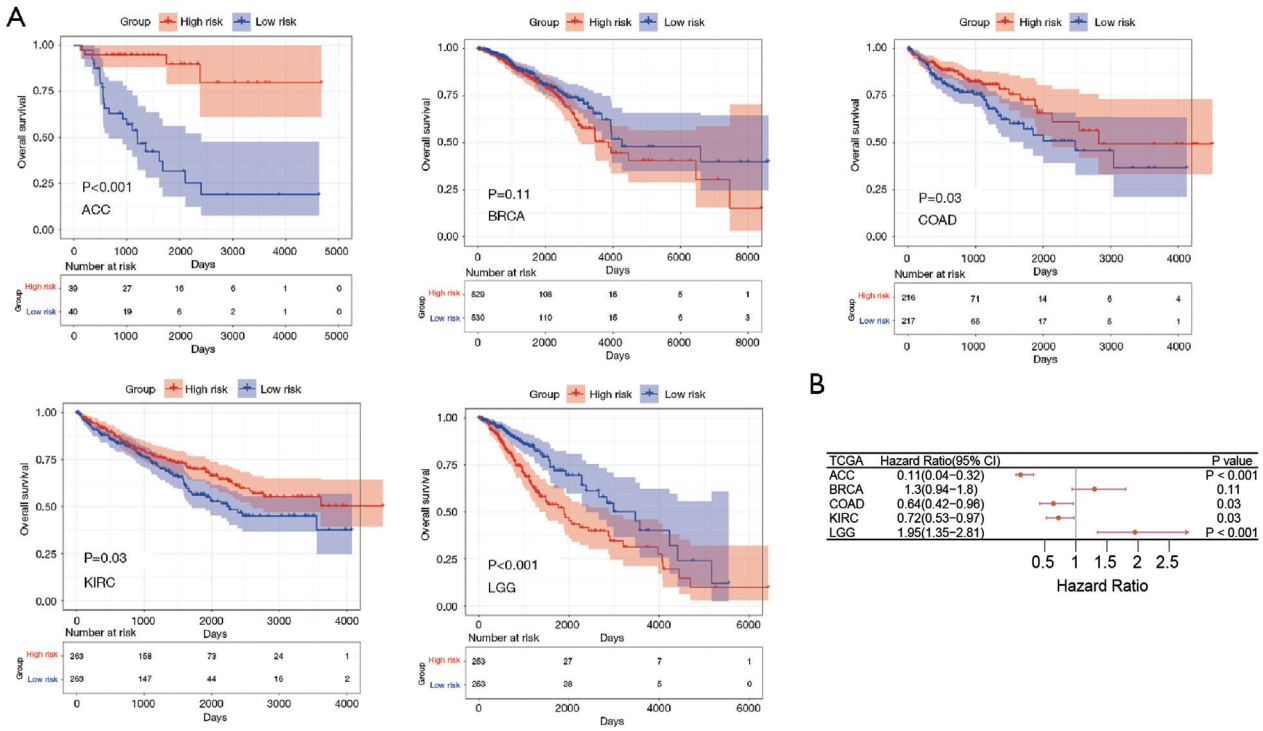

Figure S3 Pancancer analyses of OS between the high- and low-risk groups. (A) Kaplan-Meier analysis of OS in ACC, BRCA, COAD, KIRC, LGG. (B) Forest plot. TCGA, The Cancer Genome Atlas; CI, confidence interval; ACC, Adrenocortical Cancer; BRCA, Breast Cancer; COAD, Colon Adenocarcinoma; KIRC, Kidney Clear Cell Carcinoma; LGG, Lower Grade Glioma; OS, overall survival.

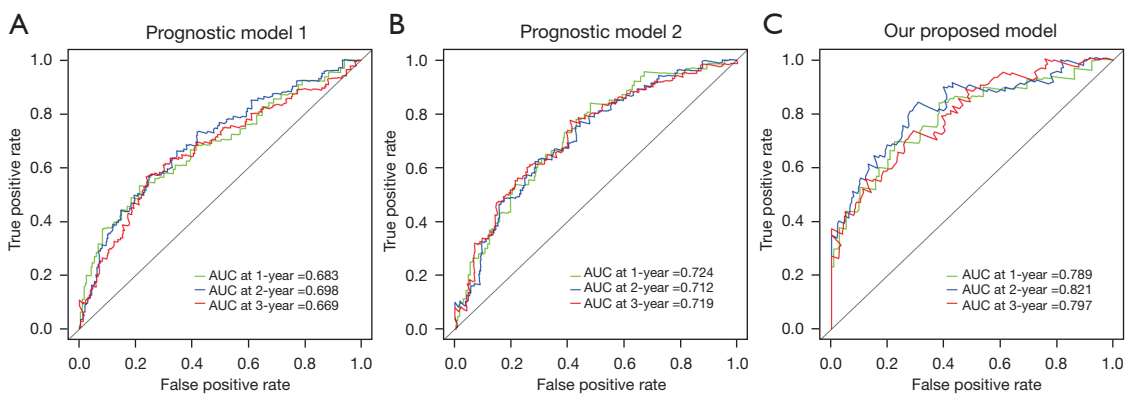

Figure S4 Our proposed model was compared with two existing RBP-related models. (A) Prognostic model 1. (B) Prognostic model 2. (C) Our proposed model. AUC, area under the curve; RBP, RNA-binding protein.

https://dx.doi.org/10.21037/tcr-2024-2561

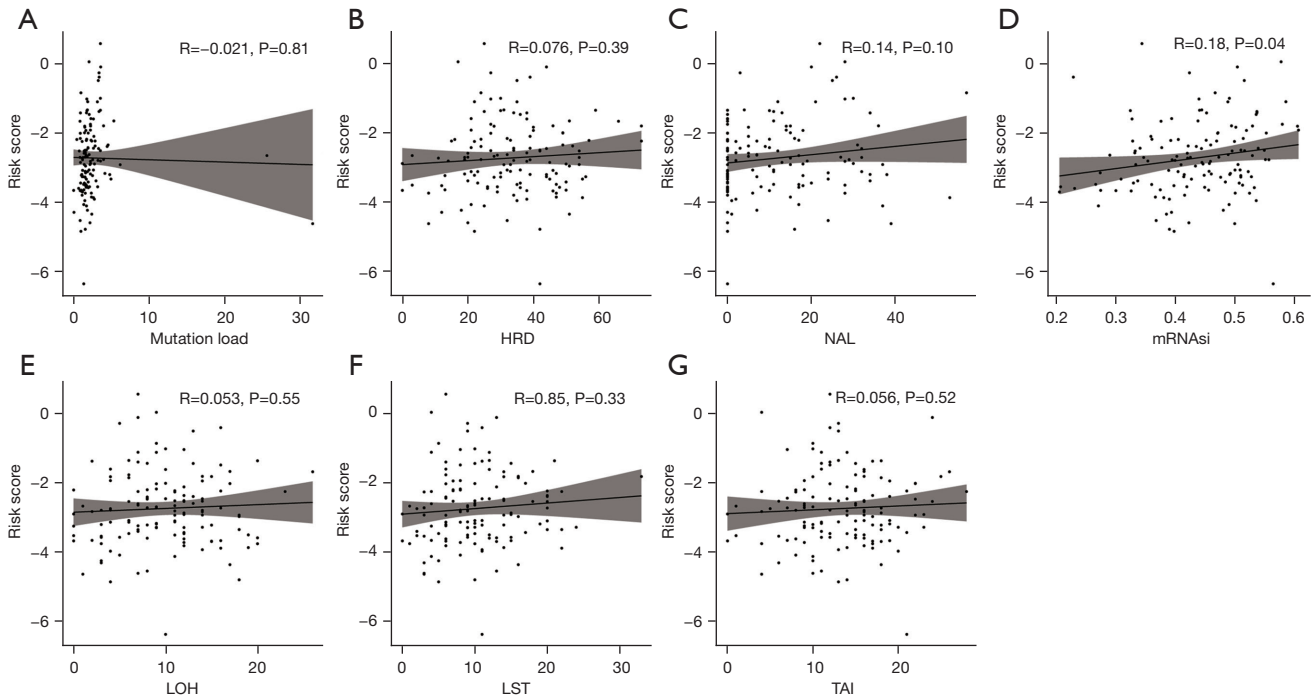

Figure S5 Relationship between the RBP risk score and biomarkers for predicting ICI response. (A) TMB. (B) HRD. (C) NAL. (D) Stemness index. (E) LOH. (F) LST. (G) TAI. TMB, tumor mutation burden; HRD, homologous recombination deficiency; NAL, neoantigen load; mRNAsi, messenger RNA expression-based stemness index; LOH, loss of heterozygosity; LST, large-scale state transition; TAI, telomeric allelic imbalance; RBP, RNA-binding protein; ICI, immune checkpoint inhibitor.

https://dx.doi.org/10.21037/tcr-2024-2561